Biochemical and Biophysical Research Communications 382 (2009) 200–204

Contents lists available at ScienceDirect

Biochemical and Biophysical Research Communications

journal homepage: www.elsevier.com/locate/ybbrc

Crystal structure of a methyltransferase from a no-known-vector *Flavivirus*

Michela Bollati [a], Mario Milani [a,b], Eloise Mastrangelo [a,b], Xavier de Lamballerie [c], Bruno Canard [d], Martino Bolognesi [a,*]

[a] Department of Biomolecular Sciences and Biotechnology, CNR-INFM and CIMAINA, University of Milano, Via Celoria 26, 20133 Milano, Italy
[b] CNR-INFM-S3 National Research Center on Nanostructure and BioSystems at Surfaces, Via Campi 213/A, 41100 Modena, Italy
[c] Unité des Virus Emergents, Faculté de Médecine, 27 Bd Jean Moulin, 13005 Marseille, France
[d] Laboratoire Architecture et Fonction des Macromolécules Biologiques, UMR 6098, AFMB-CNRS-ESIL, Case 925, 163 Avenue de Luminy, 13288 Marseille, France

ARTICLE INFO

Article history:
Received 25 February 2009
Available online 9 March 2009

Keywords:
Flavivirus
RNA capping
Methyltransferase
Viral enzyme structure

ABSTRACT

Presently known flaviviruses belong to three major evolutionary branches: tick-borne viruses, mosquito-borne viruses and viruses with no known vector. Here we present the crystal structure of the Yokose virus methyltransferase at 1.7 Å resolution, the first structure of a methyltransferase of a *Flavivirus* with no known vector. Structural comparison of three methyltransferases representative of each of the *Flavivirus* branches shows that fold and structures are closely conserved, most differences being related to surface loops flexibility. Analysis of the conserved residues throughout all the sequenced flaviviral methyltransferases reveals that, besides the central cleft hosting the substrate and cofactor binding sites, a second, almost continuous, patch is conserved and points away from active site towards the back of the protein. The high level of structural conservation in this region could be functional for the methyltransferase/RNA interaction and stabilization of the ensuing complex.

Introduction

The genus *Flavivirus* comprises over 70 viruses many of which are known to be etiological agents of human diseases. Flaviviruses are small, enveloped viruses containing a single-stranded, plus-sense RNA genome of 11 kb [1]. Phylogenetic studies revealed that the presently known flaviviruses belong to three major evolutionary branches: tick-borne flaviviruses (TBFVs), mosquito-borne flaviviruses (MBFVs) and flaviviruses with no known vector (NKVs) [2]. All flaviviruses have a similar genome organization, presenting one single large open reading frame preceded by a long 5′-untranslated region which is decorated with a cap1 structure (i.e. $^{N7Me}GpppA_{2'OMe}$-RNA). Translation of the genome yields a 370 kDa polyprotein, which is processed by viral and cellular proteases into three structural proteins and seven non-structural proteins involved in the replication of the virion (NS1, NS2A, NS2B, NS3, NS4A, NS4B, and NS5) [1]. NS5 is a large protein consisting of an N-terminal methyltransferase (MTase) and a C-terminal RNA-dependent-RNA polymerase (RdRp) domain. The MTase is involved in the formation of the mRNA cap, a structure consisting of an inverted guanosine linked to the 5′ end of viral and eukaryotic mRNA. The cap plays an essential role in the life cycle of mRNA, being required for efficient pre-mRNA splicing, export, stability and translation [3]. In order to accomplish this task, the cap needs to be decorated by addition of methyl groups to the N7 position of the guanine, and to the ribose 2′-OH group of the first nucleotide of the mRNA. In flaviviruses both steps are catalyzed by the NS5 N-terminal MTase domain which transfer a methyl group from the cofactor *S*-adenosyl-L-methionine (AdoMet) to the substrate RNA [4–6]. To date, three-dimensional structures of flaviviral MTases have been reported only for the TBFV and MBFV group. These include the following species: the TBFV Meaban virus (Mv [7]), and, within the MBFVs group, Dengue virus [8,9], Murray Valley encephalitis virus [10], West Nile virus [5], Yellow Fever virus [11], and Wesselsbron virus [12].

Here we present the 1.7 Å resolution crystal structure of Yokose virus (Yv) NS5 methyltransferase domain (^{Yv}MTase). Yv is a NKV isolated for the first time in 1971 in Japan from a bat [13]. Yv is genetically very interesting because, despite being a NKV, it is closely related to the Yellow Fever virus group [14]. Extensive crystallization trials on a long construct of ^{Yv}MTase consisting of residues 1–293 ($^{Yv}MTase_{LC}$, nomenclature according to Mastrangelo et al. [7]) yielded crystals suitable for X-ray analysis [15]. However, data collected to 2.7 Å resolution were difficult to analyze because of the excessive unit-cell size. Considering that success in the crystallization of flaviviral MTases has been related to a construct length

Abbreviations: TBFVs, tick-borne flaviviruses; MBFVs, mosquito-borne flaviviruses; NKVs, flaviviruses with no known vector; NS, non-structural protein; MTase, methyltransferase; RdRp, RNA-dependent-RNA polymerase; AdoMet, *S*-adenosyl-L-methionine; Yv, Yokose virus; Dv, Dengue virus; Mv, Meaban virus; LC, long construct; SC, short construct

* Corresponding author. Fax: +39 02 50314895.
E-mail address: martino.bolognesi@unimi.it (M. Bolognesi).

0006-291X/$ - see front matter © 2009 Elsevier Inc. All rights reserved.
doi:10.1016/j.bbrc.2009.03.008

covering residues 1–265/9 [7,10], we produced a ^{Yv}MTase short construct (^{Yv}MTase$_{SC}$; residues 1–265). In order to analyze structural differences between the MTases representative of each of the three *Flavivirus* genus, we compared ^{Yv}MTase belonging to the NKV to the TBFV ^{Mv}MTase (PDB Code: 2OXT [7]) and to the MBFV ^{Dv}MTase type 2 (PDB Code: 1R6A [8]). The structural comparison shows that the fold is closely similar in the three structures, and most differences are caused by surface loops flexibility. Analysis of the residues conserved throughout all the sequenced flaviviral methyltransferases reveals that, besides the central cleft containing the substrate and cofactor binding sites, an almost continuous patch pointing away from active site towards the back of the protein is strongly conserved.

Materials and methods

Cloning, expression, and purification. Cloning and expression of ^{Yv}MTase$_{LC}$ have been already described [15]. ^{Yv}MTase$_{SC}$ was produced by amplification of ^{Yv}MTase$_{LC}$ by PfuTurbo DNA polymerase (Stratagene) using gene-specific primers designed to encode an N-terminal His$_6$-tagged recombinant protein. The product of the PCR was subsequently inserted into a pET14b expression vector via NdeI and XhoI restriction sites. The sequencing analysis (BMR Sequencing Service, University of Padova, Italy) showed that during the PCR two mutations occurs within the ^{Yv}MTase$_{SC}$ sequence: K46E and K163R. The mutated residues were estimated to be not relevant for the enzyme activity nor for the protein fold. In fact, both residues lay far from the active site, and later superimposition of ^{Yv}MTase$_{SC}$ on ^{Mv}MTase and ^{Dv}MTase did not show backbone structure differences in the mutated regions. ^{Yv}MTase$_{SC}$ was expressed and purified following the experimental protocol used for the long construct [15]. ^{Yv}MTase$_{SC}$ was concentrated to 17 mg ml^{-1} in a medium containing CHES 10 mM, pH 9, NaCl 800 mM, and DTT 1 mM, using an Amicon Ultra centrifugal filter, and employed for crystallization and activity assays.

2′O MTase activity assays. The assays were performed in 50-μl samples containing 40 mM Tris, pH 7.5, 5 mM DTT, 5 μM AdoMet (2 μCi [^{3}H]AdoMet, Amersham Biosciences), 1 μM enzyme and 2 μM of RNA substrate. RNA substrate ^{7Me}GpppAC$_5$ was prepared as described [16]. Reactions were incubated at 30 °C. At given time intervals 12-μl samples were drawn and spotted into 96-well sample plates containing 100 μl of 20 μM AdoHcy per well to stop the reaction. The samples were then transferred to glass–fiber filtermats (DEAE filtermat, Wallac) by a Filtermat Harvester (Packard Instruments). After washing, liquid scintillation fluid was added and methylation of RNA substrates was measured in counts per minute using a Wallac MicroBeta TriLux Liquid Scintillation Counter.

Crystallization and data collection of ^{Yv}MTase$_{SC}$. Vapour-diffusion crystallization experiments were assembled using an Oryx-8 crystallization robot (Douglas Instruments, East Garston, UK). All crystallization trials were performed at 293 K. Crystals of ^{Yv}MTase$_{SC}$ in complex with AdoMet were obtained after 2 weeks at 293 K against 2% PEG 400, 1.5 M ammonium sulfate, 100 mM Hepes–Na, pH 7. A 0.4 μl droplet of the protein solution (concentrated at 17 mg ml^{-1}) containing 10 mM AdoMet, was mixed with 0.6 μl of a reservoir solution. For X-ray data collection one crystal was cryoprotected in its mother liquor supplemented with 25% glycerol, and flash frozen in a nitrogen stream.

The ^{Yv}MTase$_{SC}$ crystal in complex with the cofactor diffracted to 1.7 Å resolution using synchrotron radiation (beam line ID14-1, ESRF-Grenoble, France). The diffraction data were processed with MOSFLM [17], and intensities were merged with Scala [18]. The crystal was shown to belong to the trigonal space group $P3_1$ (or $P3_2$; $a = b = 68.9$, $c = 50.8$ Å, $\gamma = 120°$). The calculated crystal-packing coefficient ($V_M = 2.14$ Å^3 Da^{-1}) indicated the presence of one molecule in the symmetric unit, with a corresponding solvent content of 42.5%. X-ray data collection statistics are summarized in Table 1.

Structure determination and refinement. The crystal structure of ^{Yv}MTase$_{SC}$ was solved by molecular replacement (MOLREP [19]) using the ^{Dv}MTase structure as search whole model (55.3% amino acid identities; PDB Code: 1R6A [8]) devoid of the cofactor molecule. A single enzyme molecule was located in the crystal asymmetric unit, space group $P3_2$, (*R*-factor 51% at 1.7 Å resolution). The molecule was subjected to rigid-body refinement (*R*-factor 44.8%), and restrained refined using REFMAC5 [20]. A random set comprising 5% of the data was omitted from refinement for *R*-free calculation. Inspection of difference Fourier maps showed a strong residual density feature compatible with one AdoMet molecule in the asymmetric unit, which was accordingly model-built. The amino acidic sequence of the model was modified to match the ^{Yv}MTase$_{SC}$ correct sequence comprising the mutations arose during the PCR (see Cloning, expression, and purification); water molecules were manually located and fitted to the electron density using the program COOT [21]. Data collection and refinement statistics are summarized in Table 1. The stereochemical quality of the model was checked using the program PROCHECK [22]. Analysis of the Ramachandran plot showed that 100% of the non-glycine residues fall in the favorable region (Table 1). Atomic coordinates and structure factors have been deposited with the Protein Data Bank [23] with Accession Code 3GCZ.

Sequence analysis. All sequences alignments were made using the Blosum62 similarity matrix [24]. The secondary structure elements were assessed using the program DSSP [25]. Secondary structures were subsequently added to the ClustalW [26] sequence alignment. Superimpositions of the structures was performed using the on line program C-alpha Match (http://bio-info3d.cs.tau.ac.il/c_alpha_match).

Results and discussion

Functional characterization

In order to demonstrate that both the ^{Yv}MTase$_{LC}$ and the solved ^{Yv}MTase$_{SC}$ are active forms of the enzyme we performed methyltransferase activity assays. We assessed the activity of the enzyme measuring the 2′O-methyltransfer of a radiolabeled methyl group

Table 1
^{Yv}MTasesc X-ray data-collection and refinement statistics.

Data collection statistics	
Space group	$P3_2$
Unit-cell parameters (Å)	a = b = 68.9, c = 50.8, $\gamma = 120°$
Resolution limits (Å)	51–1.7 (1.79–1.7)
Mosaicity (°)	0.7
No. of unique reflections	29,342 (3984)
Completeness (%)	98.7 (91.1)
Redundancy	10.9 (8.6)
R_{merge}[a] (%)	6.5 (64.9)
Average I/σ (I)	24.6 (3.1)
Refinement statistics	
R-factor[b] (%)	16.7
R-free[c] (%)	19.8
Average *B* (Å^2)	25
R.M.S. bond lengths (Å)	0.011
R.M.S. bond angles (°)	1.367
Ramachandran plot	
Resid. in most fav. reg. (%)	93.7
Resid. in add. allow. reg. (%)	6.3
Resid. in disallow. reg. (%)	0.0

Values in parenthesis are for the high resolution shell.
[a] $R_{merge} = \Sigma|I - (I)|\Sigma I \times 100$, where I is intensity of a reflection and (I) is the average intensity.
[b] *R*-factor = $\Sigma|F_o - F_c|/\Sigma|F_o| \times 100$.
[c] *R*-free is calculated from 5% randomly selected data for cross-validation.

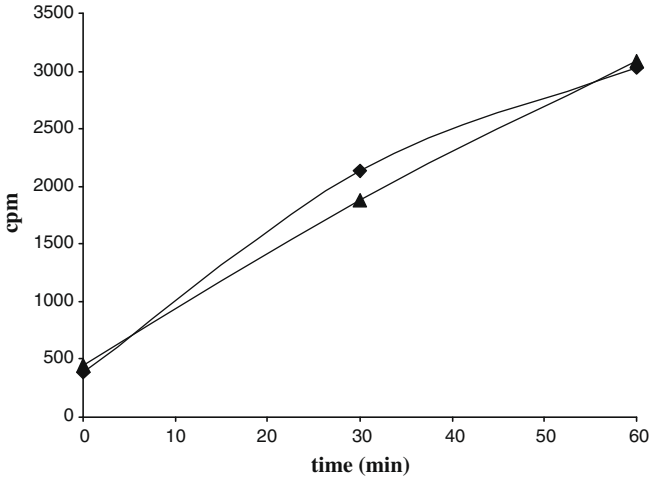

Fig. 1. 2′OMTase activity assay. Time course of methyltransfer from [^{3}H]AdoMet to three different RNA substrates followed by filter binding and liquid scintillation counting. The extent of methyltransfer from AdoMet to three different RNA substrates by ^{Yv}MTase$_{SC}$ (■) and ^{Yv}MTase$_{LC}$ (▲) is plotted as a function of time. Data points are presented as counts per minute (cpm).

from AdoMet to ^{7Me}GpppAC$_5$, a short capped RNA substrate. Both the ^{Yv}MTase$_{LC}$ and ^{Yv}MTase$_{SC}$ were shown to be active with closely similar activity (Fig. 1).

Structure of ^{Yv}MTase$_{SC}$

^{Yv}MTase$_{SC}$ (residues 1–265) was crystallized in complex with AdoMet and the structure was solved at 1.7 Å resolution. ^{Yv}MTase$_{SC}$ is a monomer characterized by an overall globular fold composed of a core domain (residues 57–223) flanked by a N-terminal region (residues 7–56), and a C-terminal region (residues 224–265). The core domain consists of a mixed and twisted seven-stranded β-sheet surrounded by four α-helices and two 3_{10}-helices (Fig. 2). This structure closely resembles the catalytic domain of all other AdoMet-dependent MTases [27,8]. The N-terminal segment comprises a helix-turn-helix motif followed by a β-strand and an α-helix. The C-terminal region consists of an α-helix and a β-strand. Relative to the AdoMet-dependent MTase consensus fold the ^{Yv}MTase$_{SC}$ structure displays two 3_{10}-helices in place of α-helices between β-strands 2 and 3 (helix GB) and β-strands 3 and 4 (helix GC). The ^{Yv}MTase core domain displays a central cleft between β-strands 1 and 4, that has been described as the active site where the cofactor AdoMet binds (Fig. 2A).

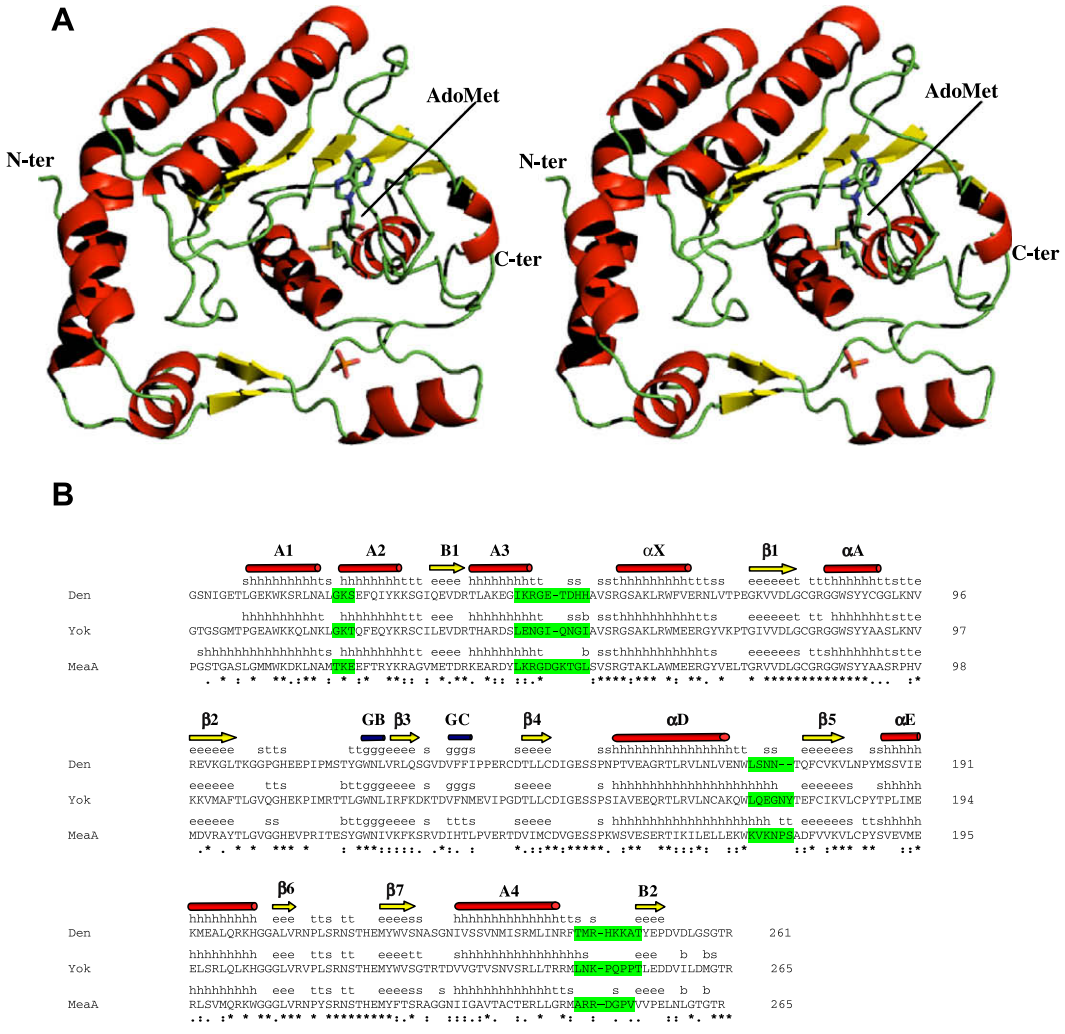

Fig. 2. (A) Stereo view of ^{Yv}MTase$_{SC}$ in complex with AdoMet. ^{Yv}MTase$_{SC}$ is a monomer characterized by an overall globular fold composed of a core domain (residues 57–223), where the cofactor AdoMet binds, flanked by a N-terminal region (residues 7–56), and a C-terminal region (residues 224–265). (B) Amino acid sequence and secondary structures alignment of ^{Yv}MTase, ^{Dv}MTase and ^{Mv}MTase. The sequence alignment was performed using the program ClustalW [26]. Secondary structures (assessed using the program DSSP [25]) were successively add to the sequence alignment.

The AdoMet-binding site

The AdoMet molecule is stabilized in the binding pocket by a network of hydrogen bonds and van der Waals contacts, generally matching those predicted as consensus interactions in AdoMet-dependent MTases [27], and involving residues well conserved within the flaviviral MTases. The adenine ring is accommodated within a hydrophobic pocket defined by the side chains of Leu105, Val132, Phe133 and Ile147, and stabilized by hydrogen bonds to the side chain of Asp131 and to the main-chain N of Val132. The AdoMet ribose moiety is stabilized by hydrogen bonds linking the 2′-OH to residue His110, being bridged via a water molecule to main-chain atoms of Gly106 and Thr104 and via a second water molecule to side chain of Glu111. The rest of the AdoMet molecule is stabilized by hydrogen bonds to the side chains of Ser56 and Asp146, to the main-chain N of Gly86, and via water molecules to Asp79, Arg84 and Trp87. The MTase active site is primarily identified by the location of the AdoMet exchangeable methyl group. Electrostatic analysis of the structure (Fig. 3D) shows an extended positively charged surface adjacent to the AdoMet-binding pocket, held to serve as RNA binding site during cap methylation. The donor-methyl group protrudes from the AdoMet pocket towards the RNA binding cleft, defining the central region of the active site [5,7,8,12].

Structural comparison of ^{Yv}MTase, ^{Mv}MTase and ^{Dv}MTase

The flaviviral MTases show a high degree of structural homology that reflects the high sequence conservation. The identities observed in the amino acid sequences of ^{Dv}MTase and ^{Mv}MTase with respect to ^{Yv}MTase are 55% (68%, considering conservative substitutions) and 49% (67%), respectively (Fig. 2B). In order to define the regions of conserved residues which could be functional for the activity and binding of the enzyme to the substrate RNA and to the cofactor AdoMet, we color coded the surface of ^{Yv}MTase (Fig. 3A–C) according to the conservation of residues, resulting from the multiple alignment of 34 sequence of flaviviral MTases (data not shown). As expected, residues involved in the capped-substrate and cofactor binding are perfectly conserved (Fig. 3A). Besides the central cleft containing these binding sites, ^{Yv}MTase surface representation shows an additional, almost continuous, conserved patch, extending away from the active site towards the back of the protein (Fig. 3B and C). It comprises a wide patch on the side of the protein, (residues Tyr89, Pro113, Gly120, Trp121, Asn122, Leu123, Ile124, Phe126, Lys127, Asp131, Gly263, Thr264 and Arg265), and a second region (residues Ala60, Trp64, Leu207, Val208, Arg209, Pro211, Met220 and Arg244) on the back of the ^{Yv}MTase (Fig. 3B and C). The analysis of the electrostatic potential shows that these regions are characterized by an overall positive charge (Fig. 3D–F). It can be speculated that the high degree of residues conservation and the positively charged patch are indicative of an MTase region playing a role in stabilizing the enzyme interaction with the RNA chain following the cap.

The rmsd deviations resulting from the superimposition between ^{Dv}MTase and ^{Mv}MTase with ^{Yv}MTase are 0.69 Å (superposing 251 residues) and 0.75 Å (considering 254 residues), respectively. Most differences are caused by loop flexibility and amino acid variability, displayed in four regiones of the enzyme: (1) helix-loop-helix motif in the guanine binding site (residues Gly21-Lys22-Thr23 in ^{Yv}MTase, substituted with Gly-Lys-Ser in ^{Dv}MTase, and Thr-Lys-Glu in ^{Mv}MTase); (2) α3–αX loop (Asn47-Ile53; insertion of one amino acid in ^{Mv}MTase); (3) αD–β5 loop

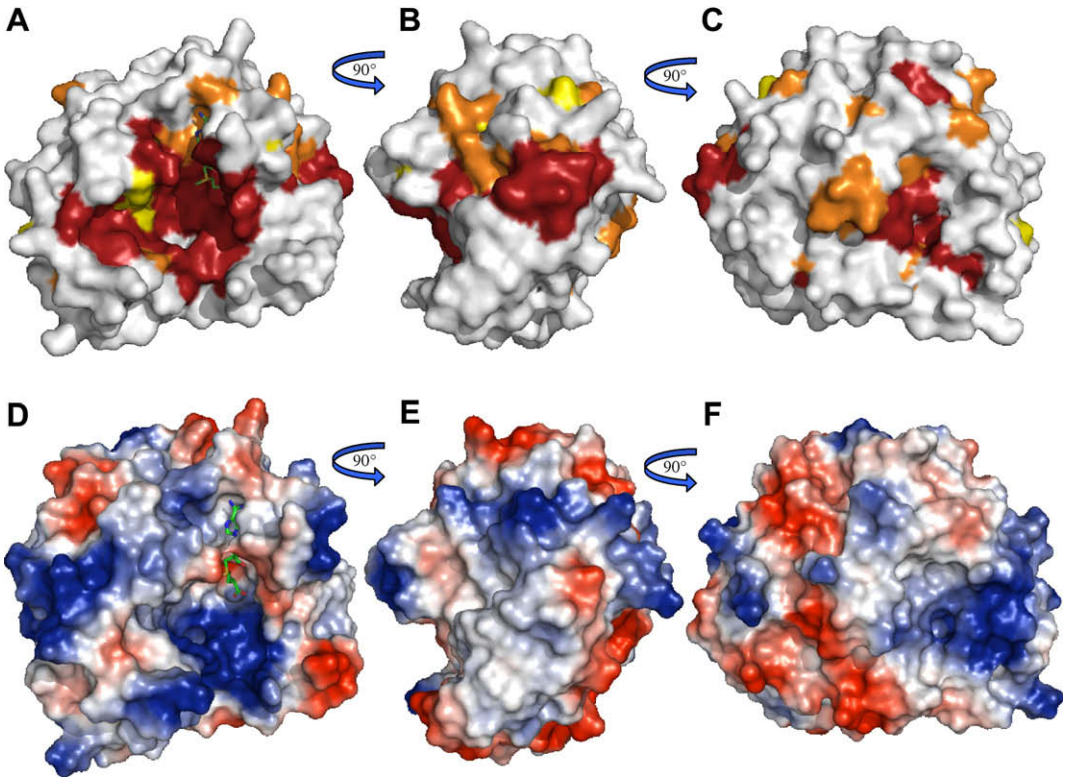

Fig. 3. Surface representations of ^{Yv}MTase$_{SC}$ viewed from three angles, differing by rotation of approximately 90° about the vertical axis: (A,D) the face containing the shallow groove where the cofactor, represented in green sticks, and the substrate bind, (B,E) the side and (C,F) the back of the molecule, opposite to the cleft face. (A–C) The surface is colored according to conserved residues, resulting from the multiple alignment of 34 sequence of flaviviral MTases: perfect match (red), low significance mismatch (score > 0.5, orange), high significance mismatch (score < 0.5, yellow), and mismatch (white). (D–F) Molecular surface color coded for the electrostatic potential. (For interpretation of the references in color in this figure legend, the reader is referred to the web version of this article.)

(Leu172-Tthr178; deletion of two amino acids in ^{Dv}MTase); and 4) α4–β8 loop (Leu246-Thr252; deletion of two amino acids in ^{Mv}MTase). Interestingly, ^{Yv}MTase B factors are about 30% higher relative to their mean value in these four regions, suggesting higher motility.

In all the structures, the cofactor AdoMet (in ^{Yv}MTase and ^{Mv}MTase), or AdoHcy (in ^{Dv}MTase), are bound to the protein. The interactions involved in AdoMet/AdoHcy binding are overall conserved in the three MTases. In particular, the hydrogen bond between Ser56 and AdoMet carboxyl group is present in all the structures, while the interaction between Asp146 and the amino group is conserved only in the ^{Yv}MTase and ^{Dv}MTase complexes. The interaction between Asp131 side chain and the adenine ring N6 atom is conserved; in ^{Mv}MTase N6 interacts also with His134 that replaces Phe in ^{Dv}MTase and ^{Yv}MTase. In general the interaction of AdoHcy to ^{Dv}MTase is weaker than AdoMet, involving fewer hydrogen bonds and van der Waals contacts. This is in agreement with the requirement for disassociation of AdoHcy (product of the methyl transfer) in favor of the binding of a new cofactor molecule.

Acknowledgments

This work has been supported by the EU IP Project Vizier (CT 2004-511960, to X.D.L., B.C. and M.B.), and by the Italian Ministry for University and Scientific Research FIRB Project "Biologia Strutturale" (to M.B.). A research grant to B.C. from the Direction Générale de l'Armement is gratefully acknowledged. We are grateful to Bruno Coutard and Karine Alvarez (Marseille) for precious technical assistance, and to Barbara Selisko for supervision during the 2′O MTase activity assays.

References

[1] T.J. Chambers, C.S. Hahn, R. Galler, C.M. Rice, Flavivirus genome organization, expression, and replication, Annu. Rev. Microbiol. 44 (1990) 649–688.
[2] M.W. Gaunt, A.A. Sall, X. de Lamballerie, A.K. Falconar, T.I. Dzhivanian, E.A. Gould, Phylogenetic relationship of flaviviruses correlate with their epidemiology, disease association and biogeography, J. Gen. Virol. 82 (2001) 1867–1876.
[3] Y. Furuichi, A. LaFiandra, A.J. Shatkin, 5′-Terminal structure and mRNA stability, Nature 266 (1977) 235–241.
[4] S. Shuman, Structure, mechanism, and evolution of the mRNA capping apparatus, Prog. Nucleic Acid Res. Mol. Biol. 66 (2001) 1–40.
[5] D. Ray, A. Shah, M. Tilgner, Y. Guo, Y. Zhao, H. Dong, T.S. Deas, Y. Zhou, H. Li, P.-Y. Shi, West Nile virus 5′-cap structure is formed by sequential guanine N-7 and ribose 2′-*O* methylations by nonstructural protein 5, J. Virol. 80 (2006) 8362–8370.
[6] Y. Zhou, D. Ray, Y. Zhao, H. Dong, S. Ren, Z. Li, Y. Guo, K.A. Bernard, P.-Y. Shi, H. Li, Structure and function of Flavivirus NS5 methyltransferase, J. Virol. 81 (2007) 3891–3903.
[7] E. Mastrangelo, M. Bollati, M. Milani, B. Selisko, F. Peyrane, B. Canard, G. Grard, X. de Lamballerie, M. Bolognesi, Structural bases for substrate recognition and activity in Meaban virus nucleoside-2′-*O*-methyltransferase, Protein Sci. 16 (2007) 1133–1145.
[8] M.P. Egloff, D. Benarroch, B. Selisko, J.L. Romette, B. Canard, An RNA cap (nucleoside-2′-*O*-)-methyltransferase in the Flavivirus RNA polymerase NS5: crystal structure and functional characterization, EMBO J. 21 (2002) 2757–2768.
[9] M.P. Egloff, E. Decroly, H. Malet, B. Selisko, D. Benarroch, F. Ferron, B. Canard, Structural and functional analysis of methylation and 5′-RNA sequence requirements of short capped RNAs by the methyltransferase domain of dengue virus NS5, J. Mol. Biol. 372 (2007) 23–36.
[10] R. Assenberg, J. Ren, A. Verma, T.S. Walter, D. Alderton, R.J. Hurrelbrink, S.D. Fuller, S. Bressanelli, R.J. Owens, D.I. Stuart, J.M. Grimes, Crystal structure of the Murray Valley encephalitis virus NS5 methyltransferase domain in complex with cap analogues, J. Gen. Virol. 88 (2007) 2228–2236.
[11] B.J. Geiss, A.A. Thompson, A.J. Andrews, R.L. Sons, H.H. Gari, S.M. Keenan, O.B. Peersen, Analysis of Flavivirus NS5 methyltransferase cap binding, J. Mol. Biol. 385 (2009) 1643–1654.
[12] M. Bollati, M. Milani, E. Mastrangelo, S. Ricagno, G. Tedeschi, S. Nonnis, E. Decroly, B. Selisko, X. de Lamballerie, B. Coutard, B. Canard, M. Bolognesi, Recognition of RNA cap in the Wesselsbron virus NS5 methyltransferase domain: implications for RNA-capping mechanisms in Flavivirus, J. Mol. Biol. 385 (2009) 140–152.
[13] S. Tajima, T. Takasaki, S. Matsuno, M. Nakajama, I. Kurane, Genetic characterization of Yokose virus, a flavivirus isolated from bat in Japan, Virology 332 (2004) 38–44.
[14] G. Grard, G. Moureaua, R.N. Charrela, J.-J. Lemassonb, J.-P. Gonzalezc, P. Galliand, T.S. Gritsune, E.C. Holmesf, E.A. Goulde, X. de Lamballerie, Genetic characterization of tick-borne flaviviruses: new insights into evolution, pathogenetic determinants and taxonomy, Virology 361 (2007) 80–92.
[15] E. Mastrangelo, M. Bollati, M. Milani, X. de Lamballerie, N. Brisbarre, K. Dalle, V. Lantez, M.P. Egloff, B. Coutard, B. Canard, E. Gould, N. Forrester, M. Bolognesi, Preliminary characterization of (nucleoside-2′-*O*-)-methyltransferase crystals from Meaban and Yokose flaviviruses, Acta Crystallogr. F62 (2006) 768–770.
[16] F. Peyrane, B. Selisko, E. Decroly, J.J. Vasseur, D. Benarroch, B. Canard, K. Alvarez, High-yield production of short GpppA- and 7MeGpppA-capped RNAs and HPLC-monitoring of methyltransfer reactions at the guanine-N7 and adenosine-2′ *O* positions, Nucleic Acid Res. 35 (2007) e26.
[17] I. Steller, R. Bolotovsky, M. Rossmann, An algorithm for automatic indexing of oscillation images using Fourier analysis, J. Appl. Crystallogr. 30 (1997) 1036–1040.
[18] Collaborative Computational Project, Number 4, The CCP4 suite: programs for protein crystallography, Acta Crystallogr. D50 (1994) 760–763.
[19] A. Vagin, A. Teplyakov, MOLREP: an automated program for molecular replacement, J. Appl. Crystallogr. 30 (1997) 1022–1025.
[20] M.D. Winn, M.N. Isupov, G.N. Murshudov, Use of TLS parameter to model anisotropic displacement in macromolecular refinement, Acta Crystallogr. D57 (2001) 122–133.
[21] P. Emsley, K. Cowtan, Coot: model-building tools for molecular graphics, Acta Crystallogr. D60 (2004) 2126–2132.
[22] R.A. Laskowski, M.W. MacArthur, D.S. Moss, J.M. Thornton, PROCHECK: a program to check the stereochemical quality of protein structures, J. Appl. Crystallogr. 26 (1993) 283–291.
[23] H.M. Berman, J. Westbrook, Z. Feng, G. Gilliland, T.N. Bhat, H. Weissig, I.N. Shindyalov, P.E. Bourne, The protein data bank, Nucleic Acid Res. 28 (2000) 235–242.
[24] S. Henikoff, J.G. Henikoff, Amino acid substitution matrices from protein blocks, Proc. Natl. Acad. Sci. USA 89 (1992) 10915–10919.
[25] W. Kabsch, C. Sander, Dictionary of protein secondary structure: pattern recognition of hydrogen-bonded and geometrical features, Biopolymers 22 (1983) 2577–2637.
[26] M.A. Larkin, G. Blackshields, N.P. Brown, R. Chenna, P.A. McGettigan, H. McWilliam, F. Valentin, I.M. Wallace, A. Wilm, R. Lopez, J.D. Thompson, T.J. Gibson, D.G. Higgins, Clustal W and Clustal X version 2.0, Bioinformatics 23 (2007) 2947–2948.
[27] E.B. Faumann, R.M. Blumental, X. Cheng, Structure and evolution of AdoMet-dependent methyltransferase, in: X. Cheng, R.M. Blumental (Eds.), S-Adenosylmethionine-Dependent Methyltransferases: Structure and Functions, World Scientific Publishing, Singapore, 1999, pp. 1–38.